(JZS) Journal of Zankoy Sulaimani,2010,13(1) Part A,(71-80)

گۆڤاری زانکۆی سلێمانی , ۲۰۱۰, بەرگ۱۳(۱) بەشی A

Analysis and Evaluation of Fresnel Zone Antenna Designs

Asaad M. Jassim Al-Hindawi*, **Ammar M. Al-Shaikly****

* Sulaimani Technical College,Sulaimani, Kurdistan Region , Iraq,

** University of Al-Nahrain,Engineering College,Baghdad, Iraq

Abstract

This paper presents an analysis and evaluation of two designs of flat aperture antenna based on Huygen's principle and Fresnel diffraction theory ; therefore, this antenna type is called Fresnel zone plate antenna. The two designs include Soret and Wood types which are different in shape, design procedure and the manufacturing techniques; thus in radiation characteristics. Using the exact solution, the radii of Fresnel zones (rings), directive gain and aperture efficiency of the antenna designs are calculated and the radiation patterns are obtained. It is found that the antenna with odd zones is better in radiation characteristics than the antenna with even zones. It is also determined that the focusing efficiency of Wood antenna design is very good and four times higher than that of Soret type. The obtained results from the two antenna designs are discussed and evaluated.

Keywords: Fresnel zone, aperture antenna, radiation pattern.

1.Introduction

The simplest Fresnel zone plate antenna is the circular half-wave zone plate invented in the nineteenth [1,2]. The basic idea is to divide a plane aperture into circular zones with respect to a chosen focal point on the basis that all reflection from each zone arrives at the focal point in phase within $\pm\pi/2$ range. If the radiation from the alternate zones is suppressed or shifted in phase by π, an approximate focus is obtained and a feed can be placed there to collect the received energy effectively. Despite its simplicity, the half-wave zone plate remained mainly as an optical device for a long time, partly because its efficiency is low and the side lobe level of its radiation is high to compete with conventional dishes and partly because antenna cost was not a crucial issue for military equipment. Following the development of Direct Broadcasting Satellite (DBS) services in the eighties, however, antenna engineers began to consider the use of Frenesel zone plates as candidate antennas for DBS reception, where the antenna cost is an important factor[3]. A British firm Mawzones Ltd. was inspired by the simplicity and ease of fabrication of zone plates and started marketing zone plate antenna products in the late 1980's [4]. This, to some extent, promoted the research on Fresenel zone antennas which the authors and their colleagues carried out between 1997-1999 at the university of Radford United Kingdom. It proved to be fruitful; several novel antenna configurations were developed, offering higher efficiency and lower side lobes [5]. Number of papers were published about the optimum design of millimeter Fresnel zone plate lens and antenna and about the focusing characteristics and properties of near half open Fresnel plate antenna and their applications [6,7].

The present paper introduces an analysis of Fresnel zone plate antenna for Soret and Wood types based on the geometrical characteristics of offset Fresnel zone. Also it studies the approaches used to calculate the radiation pattern and the effect of change of the design parameters like the focal length

E-mail: asaadalhindawi@yahoo.co.uk

and the number of rings. The results are discussed and evaluated.

2.Antenna Design

Fig.1 shows the planar Fresnel zone plates; Soret or Wood zone plate. The following sections summarize these antenna designs.

(a) Soret zone plates

Three half-open or Soret zone plate configurations are illustrated in Fig.(2). They consist of open and opaque Fresnel zone annuli[8]. In the classical microwave Soret zone plate, the opaque zone elements are thin metal rings.

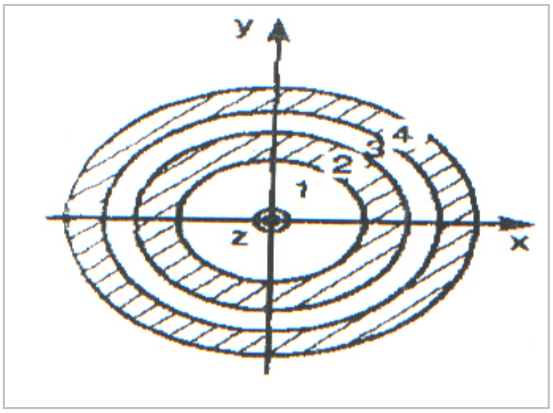

Fig.1: Planar Fresnel Soret or Wood zone plates

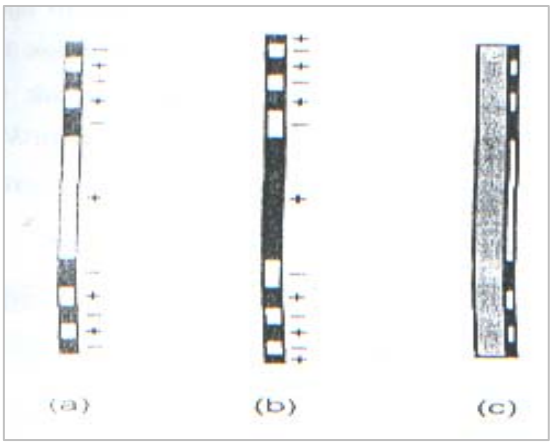

Fig. 2: Cross-sectional view of Scort zone plate
(a) metal-ring positive Soret zone plate, (b) metal-ring negative zone plate and (c) Soret zone plate with metal rings fixed on thin dielectric plate.

Depending on which Fresnel zones are open, with a positive or negative phase, the Soret zone plate is sometimes named as a positive Soret zone plate when the first ring is made from dielectric material as shown in Fig.(2a); or; a negative Fresnel zone plate when the first ring is made fom absorbing material as shown in Fig.(2b). Metal elements are usually fixed on a thin dielectric plate or substrate if the zone plate is made by printed microstrip technology (see Fig.(2c)). The focusing of the Soret zone plate is a result of two wave phenomena: diffraction by the open zone apertures and interference of diffracted waves at the focal region. Almost half of the electromagnetic energy illuminating the Soret zone plate is blocked by the opaque zones, and the phase in the open aperture is not constant. In radial direction, it varies smoothly from zero to π radian [8].

(b)Wood zone plate:

The original half-wave Wood zone plate is almost entirely transmissive for the incident light or microwave plane front[8]. It is obtained by making the Soret zone plate opaque zones transmissive and phase-reversing for the waves going through them. More precisely, in each Wood zone plate aperture, the phase also varies from zero to π radians as in the Soret zone plate. The Wood zone plate for optical or microwave/millimeter waves originated as a single-dielectric phase reversing transmission zone plate as shown in Fig.(3) a and b . The phase reversing is made by means of Fresnel zone annular grooves cut in dielectric flat plate with a permittivity ε transmissive for the light or microwaves. As a result, each groove is alternately by a dielectric rib. The Wood zone plate can be modified as a two-dielectric combination of Fresnel zone concentric rings of equal thickness (see

figure 3 c, d and e). These planar Wood zone plate varieties have the same focusing quality as the original Wood zone plate. They were proposed for microwave/millimeter waves [9].

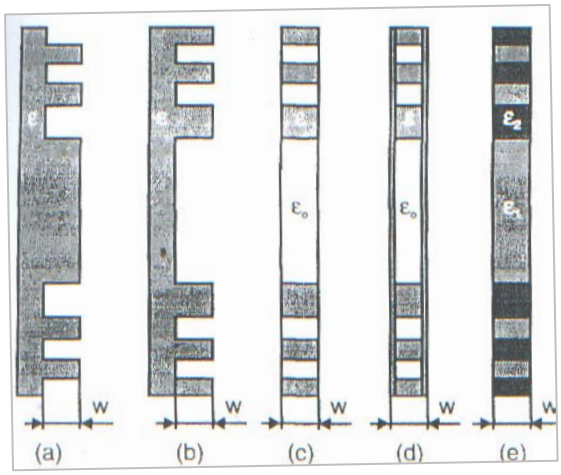

Fig.3: Wood zone plates with (a) negative-phase grooves, (b) positive-phase grooves, (c) solid rings alternated by air regions, (d) three-layer sandwich structure, and (e) two kinds of solid rings (ε_1 alternated by ε_2 rings).

3.Analysis

Fig.4 represents the geometry of Soret zone plate antenna illuminated by an axially symmetric feed field. The feed gain pattern $G_a(\psi)$ is modeled by the cosine equation [3]:

$$G_a(\psi)=\begin{cases} G_{a0}\cos^m\psi & 0\le\psi\le\frac{\pi}{2} \\ 0 & \psi>\frac{\pi}{2} \end{cases} \quad (1)$$

where $G_{a0}=G_a(\psi=0)=2(m+1)$ is the maximum antenna gain , m=1,2,3,…. is a positive number and ψ is illumination angle. Beside the axial radiation symmetry, the antenna feed has Huygens source polarization properties and the field at the zone plate in the xy-plane has an electric vector expressed as [10]:

$$\hat{E}_f(\psi,\xi,m)=C_f\sqrt{G_a(\psi,m)}\frac{e^{-j\beta_0\rho(\psi)}}{\rho(\psi)}\hat{e}_f(\psi,\xi) \quad (2)$$

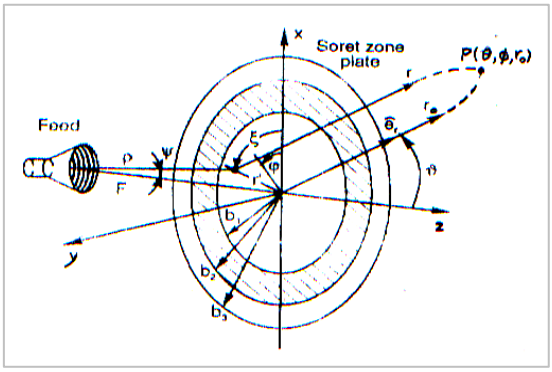

Fig.4: Geometry of Soret zone plate antenna illuminated by an axially symmetry feed field

where $C_f=(\frac{P_t\eta}{2\pi})^{0.5}$ is the amplitude constant. P_t is the feed radiation power and $\eta=\sqrt{\mu/\varepsilon}=\eta_0=120\pi$ for free space, and the polarization unit $\hat{e}_f(\psi,\xi)$ is written as:

$$\hat{e}_f(\psi,\xi)=-\cos\xi\ \hat{e}_\psi+\sin\xi\ \hat{e}_\xi \quad (3)$$

From the geometrical consideration[9]:

$$\rho(\psi)=F/\cos\psi \quad (4)$$

where F is the focal length. Now, for the zone plate illuminated by the electric vector field given in Eq.(2), the far-electric field at the observation point (p) can be expressed by transformation of the factorial Kirchhoff diffraction integral to the following [11-13]:

$$\hat{E}(\theta,\phi)=C\hat{e}_r\times\iint_s[\hat{n}\times\hat{e}_f(\psi,\xi)]\sqrt{G_a(\psi,m)}\times\frac{e^{-j\beta_0\rho(\psi)}}{\rho(\psi)}e^{j\beta(\hat{e}_r\cdot\hat{r}')}dS \quad (5)$$

where $$C=j\frac{\beta e^{-j\beta r_0}}{2\pi r_0}C_f \quad (6)$$

and the normal unit-vector $\hat{n}$ is oriented along the z-axis (ie: $\hat{n}=\hat{e}_z$). The unit polarization vector $\hat{e}_f(\psi,\xi)$ has rectangular coordinates given for short in the following matrix form[8]:

$$\hat{e}_f(\psi,\xi)=\begin{bmatrix} -\cos^2\xi\cos\psi-\sin^2\xi \\ \sin\xi\cos\xi(1-\cos\psi) \end{bmatrix} \quad (7)$$

and the vector product $\hat{n} \times \hat{e}_f(\psi,\xi)$ yields :

$$\hat{n}\times\hat{e}_f(\psi,\xi)=\begin{bmatrix}(\cos\psi-1)\sin\xi\cos\xi\\ -\cos^2\xi\cos\psi-\sin^2\xi\end{bmatrix} \quad (8)$$

reversing transmission zone plate as shown in Fig.3a and b. The phase reversing is made by the unit vector $\hat{e}_r(\theta,\phi)$ points to far-field region and its rectangular components are given by:

$$\hat{e}_r(\theta,\phi)=\begin{bmatrix}\sin\theta\cos\phi\\ \sin\theta\sin\phi\\ \cos\theta\end{bmatrix} \quad (9)$$

The vector $\hat{r}$ defines the position of the elementary area $d\hat{S}$ point on the zone plate plane and can be written as:

$$\hat{r}=\begin{bmatrix}F\tan\psi\cos\psi\\ F\tan\psi\sin\psi\\ 0\end{bmatrix} \quad (10)$$

The aperture elementary area $d\hat{S}$ is easily found as :

$$d\hat{S}=\frac{F^2\tan\psi}{\cos^2\psi} \quad (11)$$

The scalar product in the phase factor $e^{j\beta(\hat{e}_r\cdot\hat{r})}$ is given by :

$$\hat{e}_r\cdot\hat{r}=F\sin\theta\tan\psi\cos(\phi,\xi) \quad (12)$$

After substituting Eqs. (11) and (12) into (5) and carrying out the ξ-integration in closed form, only ψ-integration remains. Finally the components E_θ and E_ϕ of the total far-field vector are obtained:

$$E_\theta(\theta,\phi)=-\pi C\cos\phi\sum_n\int_{\psi_{n-1}}^{\psi_n}O(\psi,m)e^{M(\psi)}\times I_\theta(\theta,\psi)d\psi \quad (13)$$

$$E_\phi(\theta,\phi)=-\pi C\cos\theta\sin\phi\sum_n\int_{\psi_{n-1}}^{\psi_n}O(\psi,m)e^{M(\psi)}\times I_\phi(\theta,\psi)d\psi \quad (14)$$

where:

$$O(\psi,m)=\sqrt{G_a(\psi,m)}\,\frac{F\tan\psi}{\cos\psi} \quad (15)$$

$$M(\psi)=-j\beta F/\cos\psi \quad (16)$$

$$\psi_n=\arctan(b_n/F) \quad (17)$$

where n=1,2,…,N; is the ring number, N: total no. of zones and b_n is radius of nth ring and :

$$I_\theta(\theta,\psi)=-(\cos\psi+1)J_0(R(\theta,\psi))+(\cos\psi-1)J_2(R(\theta,\psi)) \quad (18)$$

$$I_\phi(\theta,\psi)=(\cos\psi+1)J_0(R(\theta,\psi))+(\cos\psi-1)J_2(R(\theta,\psi)) \quad (19)$$

and

$$R(\theta,\psi)=\beta F\sin\theta\tan\psi \quad (20)$$

The antenna directive gain can be calculated from[10]:

$$G(\theta,\phi)=10\log\left(\frac{2\pi r^2}{\eta_0 P_t}\left|\hat{E}(\theta,\phi)\right|^2\right) \quad (21)$$

where $\hat{E}(\theta,\phi)$ is the electric far-field and is expressed as:

$$\hat{E}(\theta,\phi)=E_\theta(\theta,\phi)+E_\phi(\theta,\phi) \quad (22)$$

Far-field of Wood zone plate antenna:

The Soret zone plate illustrated in Fig.4 can be modified into a phase-reversal one simply by the metal/absorbing rings by phase–reversed dielectric or dielectric like rings. As a result, each full-wave zone will consist of a free-space inner half-wave zone with ε_{r_1} and a solid dielectric ring with ε_{r_2} filling the out half-wave zone. In this zone plate, the half-wave thickness (d) is given by[14]:

$$d=\lambda/(2(\sqrt{\varepsilon_{r_2}}-\sqrt{\varepsilon_{r_1}})) \quad (23)$$

For normal incidence, the dielectric plate with permittivity ε_{r_1} becomes fully transparent for

$$d=k\lambda/(2\sqrt{\varepsilon_{r_1}}) \quad (24)$$

where (k=1,2,3,…….) accounts for the number of standing half-waves in the dielectric medium . From Eq.(24) it is obtained that:

$$\sqrt{\varepsilon_{r_1}} = k\lambda/(2d) \qquad (25)$$

Putting Eq.(25) into (23) we get:

$$d = (k+1)\lambda/(2\sqrt{\varepsilon_{r_2}}) \qquad (26)$$

From (25) and (26), a relationship between ε_{r_1} and ε_{r_2} is easily found[15]:

$$\varepsilon_{r_2} = \varepsilon_{r_1}(\frac{k+1}{k})^2 \qquad (27)$$

The feed of axially symmetric pattern is supposed by the model given in Eq.(1) and the incident free-space ray $\rho(\psi)$ associated with the spherical wave extended through the phase-correcting dielectric ring as refraction ray. The focal distance-to-aperture diameter ratio is assumed to be large enough that the incident spherical wave is treated as a local plane wave. Ray tracing through the Fresnel zone comprising solid-dielectric and air-transparent zones is illustrated in Fig.5. The vectorial field at the input plane $I-I'$ (point Q') is given by Eq.(2). At point Q'' in the output or aperture plane $II-II'$ the refracted ray gives rise to an electric field $E_d(\psi,\xi,m)$ and can be expressed as [15,16]:

$$E_d(\psi,\xi,m) = C_f\sqrt{G_a(\psi,m)}\frac{e^{-j\beta\rho(\psi)}}{\rho''(\psi)}\hat{P}_d(\psi,\xi) \qquad (28)$$

where

$$\hat{P}_d(\psi,\xi) = -T^{\mapsto}\cos\xi\ \ \hat{e}_\psi + T^{\perp}\sin\xi\ \ e_\xi \qquad (29)$$

and $T^{\mapsto}$, $T^{\perp}$ are the multiple complex transmission coefficients for the wave of parallel, perpendicular polarization respectively through the dielectric ring. If the multiple reflection transmission coefficient of dielectric ring is approximately assumed to be the same as that of the infinite dielectric plate and for particular case, the zone plate thickness is

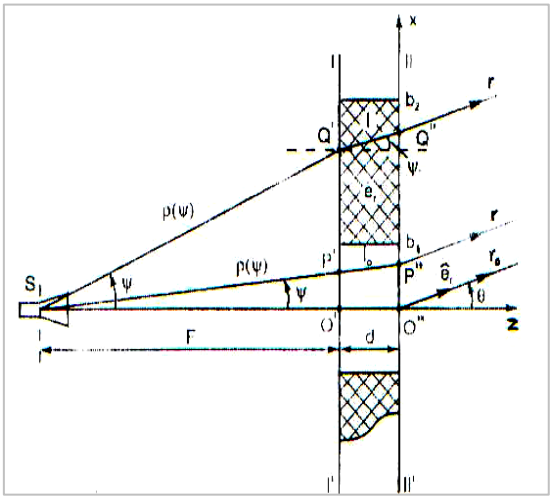

Fig. 5: Ray tracing through solid-dielectric/air-transparent zone plate (Wood zone plate).

chosen, equal to $\lambda/2$, then transmission coefficients become: $T = T^{\mapsto} = T^{\perp} = \dfrac{e^{-j\pi\sqrt{\varepsilon_r}}(1-x)}{(1-x)e^{-j2\pi\sqrt{\varepsilon_r}}}$ (30)

where $x = (\dfrac{1-\sqrt{\varepsilon_r}}{1+\sqrt{\varepsilon_r}})^2$. Now, the amplitude divergence factor $1/\rho''(\psi)$ may be expressed as[14]:

$$\frac{1}{\rho''(\psi)} = \frac{F+d}{\cos\psi} \qquad (31)$$

Putting $\rho(\psi)$ and $\rho''(\psi)$ from Eq.(4) and (31)respectively into Eq.(28) and it becomes:

$$\hat{E}_d(\psi,\xi,m) = C_f\, g\sqrt{Ga(\psi,m)}\cos\psi\hat{P}_d(\psi,\xi) \qquad (32)$$

where $g = \dfrac{e^{-j\beta F/\cos\psi}}{F+d}$, Eq.(32) gives the vector field distribution over the dielectric zone aperture. It accounts for the amplitude, phase and polarization changes due to the multiple transmission (refraction) process. The far-field vector

radiated by a dielectric aperture can be calculated as:

$$\hat{E}_d(\theta,\phi)=C\hat{e}_r(\theta,\phi)\times\iint_S\left[\hat{n}\times\hat{P}_d(\psi,\xi)\right]\cos\psi\frac{\sqrt{G_a(\psi,m)}}{F+d}\times e^{-j\beta\rho(\psi)}e^{-j\beta(\hat{e}\cdot\hat{r}')}dS' \quad (33)$$

The vector product $\hat{n}\times\hat{P}_d(\psi,\xi)$ projected in a rectangular coordinate system can be represented in matrix form:

$$\hat{n}\times\hat{P}_d(\psi,\xi)=\begin{bmatrix}(T^{\mapsto}\cos\psi-T^{\perp})\sin\xi\cos\xi\\-T^{\mapsto}\cos^2\xi\cos\psi-T^{\perp}\sin\xi\end{bmatrix} \quad (34)$$

The unit vector $\hat{e}_r(\theta,\phi)$, the vector $\hat{r}'$, the aperture elementary surface dS' and the phase factor $e^{-j\beta(\hat{e}\cdot\hat{r}')}$ are the same as in the previous sections. After setting :

$$M_d(\psi)=-j\beta L(\psi) \quad (35)$$

$$R_d(\theta,\psi)=\beta\sin\theta\left[F\tan\psi+\frac{\varepsilon_r d\sin\psi}{\sqrt{\varepsilon_r-\sin^2\psi}}\right] \quad (36)$$

$$O_d(\psi,m)=\sqrt{G_a(\psi,m)}\frac{F^2\tan\psi}{(F+d)\cos\psi} \quad (37)$$

and performing ξ-integration in a closed form, the spherical components of the far-field vector $\hat{E}_d(\theta,\phi)$ due to all dielectric apertures are:

$$E_\theta^d(\theta,\phi)=-\pi C\cos\phi\sum_n\int_{\psi_{n-1}}^{\psi_n}O_d(\psi,m)e^{M_d}I_\theta^{(d)}(\theta,\psi)d\psi \quad (38)$$

$$E_\phi^d(\theta,\phi)=-\pi C\sin\phi\cos\theta\sum_n\int_{\psi_{n-1}}^{\psi_n}O_d(\psi,m)e^{M_d}I_\phi^{(d)}(\theta,\psi)d\psi$$

where

$$I_\theta^d(\theta,\phi)=-(T^{\mapsto}\cos\psi+T^{\perp})J_0(R_d(\theta,\phi))+(T^{\mapsto}\cos\psi-T^{\perp})J_2(R_d(\theta,\phi)) \quad (40)$$

and

$$I_\phi^d(\theta,\phi)=(T^{\mapsto}\cos\psi+T^{\perp})J_0(R_d(\theta,\psi))+(T^{\mapsto}\cos\psi-T^{\perp})J_2(R_d(\theta,\phi)) \quad (41)$$

Finally, the total far-field components are found :

$$\hat{E}_\theta(\theta,\phi)=\hat{E}_\theta^{(0)}(\theta,\phi)+\hat{E}_\theta^{d}(\theta,\phi) \quad (42)$$

$$\hat{E}\phi(\theta,\phi)=\hat{E}_\phi^{(0)}(\theta,\phi)+\hat{E}_\phi^{d}(\theta,\phi) \quad (43)$$

where $\hat{E}^{(0)}{}_{(\theta,\phi)}$ referred to the far-field component radiated by air-transparent apertures that are given by Eqs.(13) to (20); with replacing F by F+d only. The antenna aperture efficiency η_{ap} can be expressed as:

$$\eta_{ap}=\frac{D_o}{(\frac{4\pi D}{\lambda})^2} \quad (44)$$

where D_o represents the antenna directivity and is given by[8]:

$$D_o=\frac{4\pi U(\theta,\varphi)}{P_{rad}} \quad (45)$$

where $U(\theta,\varphi)$ is the radiation intensity ($\frac{W}{\Omega}$) and P_{rad} is the total radiated power and D is the diameter of antenna aperture.

The radiation intensity can be calculated as:

$$U(\theta,\varphi)=\frac{r^2}{2\eta_o}\left|\hat{E}(\theta,\varphi)\right|^2 \quad (46)$$

where $\hat{E}(\theta,\varphi)$ is given by eq.(22).

4. Results and Discussion

(a) In order to understand the effects of the design parameters (like N, F, D and frequency) on the radiation characteristics, theoretical study is achieved for different numerical examples cases using Eq.[22] to calculate the field pattern of Soret type assuming the operating frequency (f=11.1GHz), the focal length (F=2m) and the umber of Fresnel zones (N=5; odd zones). The aperture diameter is chosen as D=1.14m so that it is approximately equal to the diameter of the last ring . Since the change in the angle ϕ has no effect because the shape of the antenna is circular, it is assumed $\phi = 45^0$. Feed radiation power P_t is chosen equal to be one unit and the value of r is selected to satisfy the condition of the far region. The

shapes of the radiation pattern for the given parameters are found for N= 5,6,7,9 and these results are summarized in Table.1. Some of the shapes of those patterns are plotted in Fig.6 , Fig.7 and Fig.8 for N= 5,9 and 6 respectively. The change of the gain, the directivity and the efficiency with respect to number of zones is found and shown in Fig.9 . It can be noticed that the gain, the directivity and the efficiency increase as the number of zones (even or odd) is increased, but the values of the gain, the directivity and the efficiency for the odd zones greater than those for the even zones.

(b)Using Eqs.(42), (43) , the radiation characteristics of the Wood type are found for $\varepsilon_{r_1}=1$ and $\varepsilon_{r_2}=4$.

Table 1: Summary of the obtained results for Sort type.

N	D meter	3dB degree	SLL dB	Directive Gain dB	Efficiency η_{ap} %
5	1.14	1.5	-15.7	28.2	8.84
6	1.15	1.5	-13.2	27.9	6.90
7	1.24	1.3	-17.9	30.4	10.48
9	1.41	1.2	-19.6	32.1	11.86

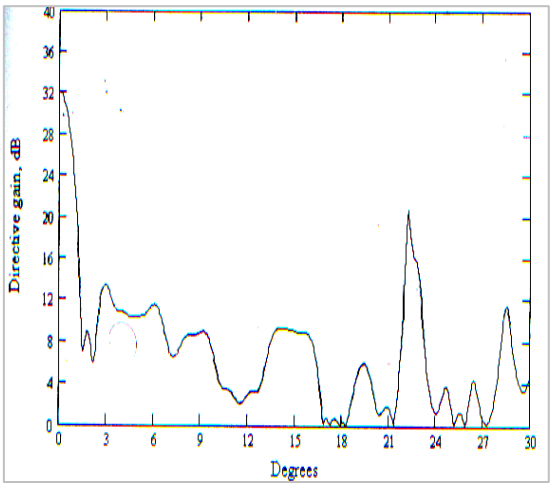

Fig.6: Directive gain of Soret type with 5 zones(3 transparent/ 2 absorbing).

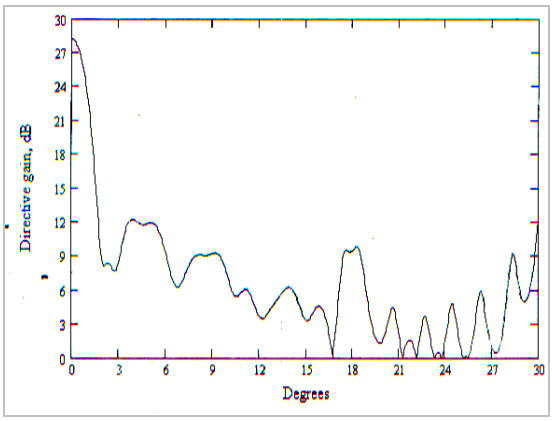

Fig.7: Directive gain of Soret type with 9 zones (5 transparent/ 4 absorbing).

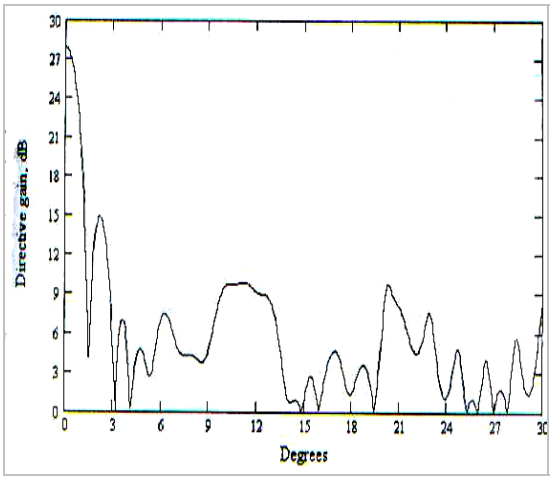

Fig.8: Directive gain of Soret type with 6 zones (3 transparent/ 3 absorbing).

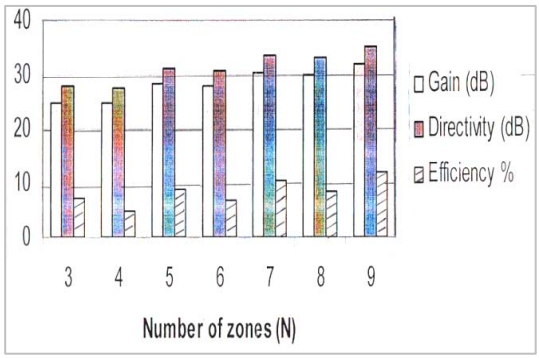

Fig.9: Change of gain, directivity and efficiency with respect to the number of zones (odd and even) for Soret type.

The radiation patterns for N=5,6,7 and 9 are obtained and the results are also summarized in Table 2. Some of the patterns are plotted in Fig.10, Fig.11 and

Fig.(12) for N=5,9 and 6 respectively. Also the response of the gain, the directivity and the efficiency with respect to zone number is illustrated in Fig.13 .

Table 2: Summary of the obtained results for Wood type.

N	D meter	3dB degree	SLL dB	Directive Gain dB	Efficiency η_{ap} %
5	1.14	1.5	-14.7	34.2	35.38
6	1.15	1.3	-12.8	33.8	27.12
7	1.24	1.3	-18.4	36.4	42.88
9	1.41	1.2	-20.2	38.2	46.60

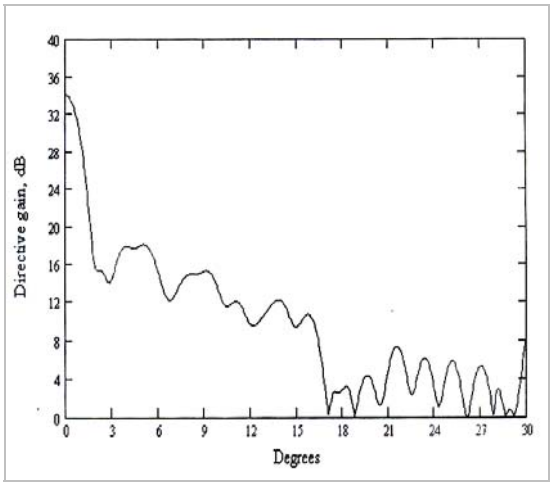

Fig.10: Directive gain of Wood type with 5 zones(3 transparent/ 2 absorbing).

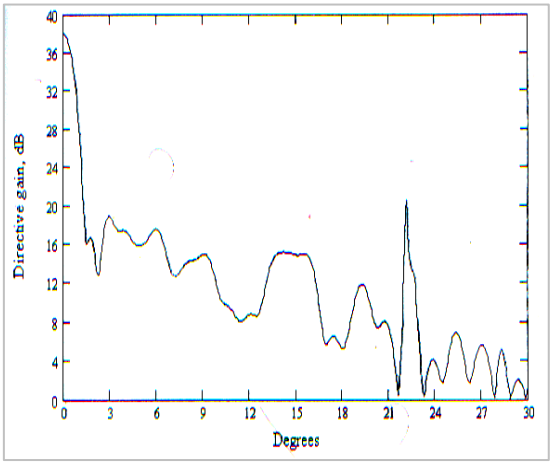

Fig.11: Directive gain of Wood type with 9 ones (5 transparent/ 4 absorbing).

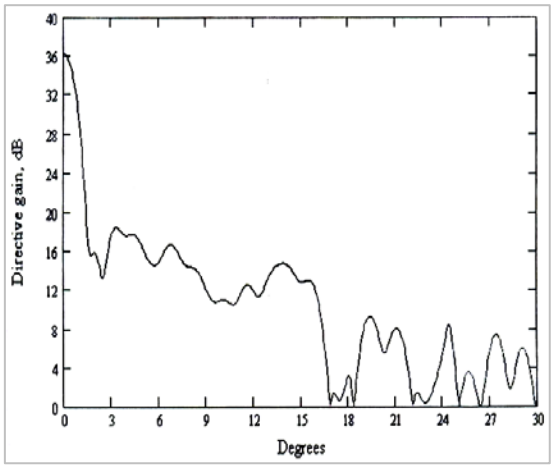

Fig.12: Directive gain of Wood type with 6 ones (3 transparent/ 3 absorbing).

It can be seen that (from Tables 1 and 2), for the Wood type, the aperture efficiency is very good and four times higher than that of Soret type and the antennas with odd zones is better in gain, efficiency and side lobe levels (SLL) as compared with those of antennas with even zones.

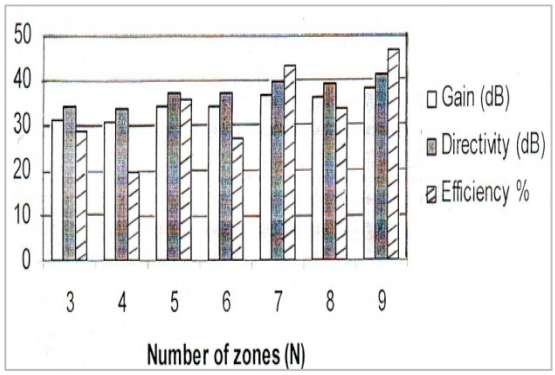

Fig.13: Change of gain, directivity and fficiency with respect to the number of zones(odd and even) for Wood type.

5. Conclusions

The radiation characteristics of Fresnel zone plate antenna are analyzed for both Soret and Wood designs. The focusing efficiency of the Wood zone plate is found four time higher than the Soret efficiency. The Wood zone plate has much reduced thickness, weight and dielectric losses compared to traditional dielectric lens.

References

1. Wood R. W., " Phase-revalsal zone plates and diffract telescopes",*Phil Mag*.,S5, June **1898,** 45 (277), 511-523.
2. Garret J. E. and Wiltse J. C., "Fresnel zone plate antenna at millimeter wavelength", *Int. Journal of Infrared and Millimeter Waves*, Dec.**1991,** 12 (3), 195-216.
3. Shuter W. L. H. and Chan C.P., Li E.W.P. and A. K. C " A metal plate Fresnel lens for 4GHz satellite TV reception ", *IEEE Trans. Antennas Propagate.* , March **1984,** AP-32 (3), 306-307.
4. Lambley R. ,"Fresnel antenna", Electronics and Wireless World , August **1989,** 792.
5. Jay Y. and Barton K.,"Fresnel zone plate antenna", Mobisphere Ltd., Boston **2002**.
6. Openning for researchers in the area of wireless communition Universidad Tecnica Federico Santa Maria,www.utfsm.cl.
7. Reid D. R. and Smith G. S.,"A Comparison of the Focusing Properties of Fresnel Zone Plate With a Doubly-Hyperbolic Lens for Application in a Free-Space, Focused-Beam Measurement System",*IEEE Trans. on Antannas and Propagation*, Feb. **2009,** 57 (2).
8. Hristov, H.D. "Fresnel zones in wireless links , zone plate lenses and antennas", Artech House, **2000**.
9. Wiltse J. C. ,"The phase correcting zone plate",Proc. Int. Conf. Infrared Millimeter Waves, Lake Buena Vista, FL, **1985,** 345-347.
10. Hristov H., Kirov G., Urumov J., Nedelchev I.,"Miniaturization of microwave antenna for satellite communication",Technical Report, Varna Technical University, Bulgaria **1998**.
11. Lyten L. "Fresnel zone plate antenna versus parabolic reflecter antenna",Technical Report, Eindhoven Univ. Technology, April **1991**.
12. Leyten L. and Herben M. "Vectorial far field of the Fresnel zone plate antenna", *IEEE Trans. Micro. Theor.and Tech.*, **1992,** 5 (2), 49-56.
13. Balanis C., " Advance engineering electromagnetics", New York ,John Wiley , **1989**.
14. Personal communication with Dr. Hristo Hristov, **2005**.
15. Hristov H. ,"Millimeter wave Fresnel zone Plate lens and antenna" , *IEEE Trans. Micro.Theory Tech.*, Dec.**1995,** 43, 2770-2785.
16. Houten V. and Herben M., "Analysis of phase correcting Fresnel zone plate antenna with dielectric/transparent zones", *J .Electromagnetic Waves and Applications*, **1994,** 8 (7), 746-749.

شی کردنەوە وهەڵسەنگاندنی ئەنتێنای (فێرنل)

أسعد الهنداوی* , عمار الشێخلی** .

*کۆلێجی تەکنیکی سلێمانی / هەرێمی کوردستان / عیراق .

** کۆلێجی ئەندازیاری / زانکۆی نە هرێن/بغداد / عیراق .

پوختــــە

ئەم تۆژینەوەیە شیکاری وهەڵسەنگاندن پێشکەش دەکات بۆ دوودیزاینی جیا جیا کە یەکێکیان بریتی یە لە :ئە نتێنای کونی داتاشراو (الفتحه المسگحه) کە لە سەر بۆچوونی (هایکن) کاری پی کراوە , وەبیردۆزەی (فیرنل) کە ئەمیش پێ ی ئەوترێ ئەنتیناکانی ئەڵقەکانی (فیرنل) هەردوو دیزاینەکەی ئەنتینای جۆری(سۆرت) وئەنتێنای جۆری (وود) ی تیا بدی ئەکرێ کە ئەوانیش لە ڕواڵەتی شێوەوجیاوازان چ لە ڕووی ڕێگای دیزاین کردنی , تەکنیکی دروستکردن وەهەروەها تایبە تمەندی تیشکدانەوە. بە بەکارهێنانی چارەسەری ڕێك و پێك نیوەتیرەی ئەڵقەکانی (فێرنل) حساب کرا ,فاکتۆری گەورەکردن, توانای هەر ئەنتێنایەك دراسەکراوە , دەر ئە نجام دەرکەت کەوا ئەنتێنای ئەڵقەی تاك باشترە لە ئەنتێنای ئەڵقەی جوت لە ناحیە تایبە تمەندی ئیشدانەوەدا . هەروەها دەرچوو کە توانای ئەنتینای (وود) زۆر باشە وچوار جار بەرزترە لەوەی کە ئەنتێنای (سۆرت) هەیەتی. دوایش ئەو ئە نجامامانەی لەم تۆژینەوەدا بە دەست هاتیون تاو تۆی کراوە هەڵسەنگینرا ..

تحليل وتقييم تصاميم هوائيات (فرنل)

أسعد الهنداوي* , عمار الشيخلي**

*الكلية التقنية في السليمانية/ أقليم كردستان / العراق .

** كلية الهندسة / جامعة النهرين / بغداد / العراق .

الخلاصة

تقدم هذه المقالة تحليلا وتقييما لتصميمين من هوائيات الفتحة المسطحة والمعتمدة على مبدأ (هايكن) ونظرية (فرنل), حيث تسمى بهوائيات حلقات (فرنل). يتضمن التصميمان هوائي نوع (سورت) وهوائي نوع (وود) اللذان يختلفان من ناحية الشكل , طريقة التصميم وتقنيات التصنيع وكذلك في خواصهما الأشعاعية. بأستخدام الحل المضبوط تم حساب أنصاف أقطار حلقات (فرنل) , معلمل التكبير وكفاءة كل هوائي مدروس وكذلك تم الحصول على الخواص الأشعاعية لهما. لقد وجد بأن الهوائي ذو الحلقات المفردة أفضل بالخواص الأشعاعية من ذلك الهوائي ذي الحلقات الزوجية. وقد وجد أيضا أن كفاءة هوائي(وود) جيدة جدا و أربعة مرات أعلى من تلك التي لهوائي (سورت). تم مناقشة وتقييم النتائج المستحصلة من هذه الدراسة.

وەرگیراوە لە ٢٠٠٩/٧/٢ دا , و پەسەند کرا لە ٢٠١٠/٦/٢٨ دا

Received 2/7/2009 , Accepted 28/6/2010